December, 2011

Thermodynamics and phase transitions for the Heisenberg model on the pinwheel distorted kagome lattice

Ehsan Khatami, *Georgetown University*
Rajiv R.P. Singh, *University of California, Davis*
Marcos Rigol, *Georgetown University*

Thermodynamics and phase transitions for the Heisenberg model on the pinwheel distorted kagome lattice

Ehsan Khatami,[1] Rajiv R. P. Singh,[2] and Marcos Rigol[1]

[1]*Department of Physics, Georgetown University, Washington, D.C. 20057, USA*
[2]*Physics Department, University of California, Davis, California 95616, USA*

We study the Heisenberg model on the pinwheel distorted kagome lattice as observed in the material $Rb_2Cu_3SnF_{12}$. Experimentally relevant thermodynamic properties at finite temperatures are computed utilizing numerical linked-cluster expansions. We also develop a Lanczos-based, zero-temperature, numerical linked-cluster expansion to study the approach of the pinwheel distorted lattice to the uniform kagome-lattice Heisenberg model. We find strong evidence for a phase transition before the uniform limit is reached, implying that the ground state of the kagome-lattice Heisenberg model is likely not pinwheel dimerized and is stable to finite pinwheel-dimerizing perturbations.

I. INTRODUCTION

Among all of the realistic quantum spin models studied to date, the spin-half kagome-lattice Heisenberg model (KLHM) stands out as one with perhaps the most esoteric low-energy properties.[1] The classical Heisenberg model on this lattice of corner-sharing triangles has an exponentially large number of ground states. Fluctuations lead to a selection of $\sqrt{3} \times \sqrt{3}$ order.[2] However, such an order is clearly absent in the spin-half model.[3] A comparison between exact diagonalization (ED) results in different lattice geometries highlights the unusual spin physics of this model.[1] Square and triangular lattice models show a tower of rotor states separated from the rest of the spectrum, as expected for a system with spontaneously broken spin-rotational symmetry. In contrast, the KLHM shows that (i) the energy gaps are an order of magnitude smaller than on the other lattices, and (ii) there are a very large number of low-lying singlet states. These data have been interpreted to support the existence of (i) a very small or even zero triplet gap,[4] (ii) gapless singlet excitations,[5] and (iii) an exponentially large number of singlets below the lowest triplet.[6]

Numerical and analytical studies have suggested alternative ground states, which include several different valence-bond crystals (VBCs), as well as gapped and gapless resonating valence-bond (RVB) spin liquids.[6–10] Most numerical studies, including the recent density matrix renormalization group (DMRG) study of Yan *et al.*,[10] suggest a singlet ground state with a gap to spin excitations in the thermodynamic limit. While earlier numerical studies[1] provided evidence for a spin gap of the order of $J/20$, where J is the nearest-neighbor exchange constant, and a much smaller gap to singlet excitations (possibly even gapless), recent DMRG work puts the singlet gap at $0.05J$, with a larger gap for the triplets. These studies should be contrasted with the experimental results for the KLHM.[11–13] Among them, the herbertsmithites with structurally perfect kagome planes have attracted the most interest. The experimental data for these systems show no evidence of a spin gap. However, substitutional impurities and Dzyaloshinskii-Moria anisotropy are present in these systems and may be playing a role in producing the eventual thermodynamic phase.[14,15]

One kagome material that does show gapped spin excitations is $Rb_2Cu_3SnF_{12}$.[16,17] This material also has substantial pinwheel distortions, which results in a 12-site unit cell[9] and four different nearest-neighbor exchange constants, with the ratio of the largest to smallest being about two (see Fig. 1). Given the many theoretical proposals for spin-gapped and VBC phases for the KLHM and this experimental finding, it is natural to ask if the uniform KLHM has a tendency to spontaneously dimerize in this pattern.

Here, we study this possibility and the role such a pattern of distortion might play in the ground state of the uniform KLHM. In earlier series-expansion studies, different dimer configurations were studied order by order in powers of a parameter λ, which takes one from a dimerized to a uniform Hamiltonian.[8] In each successive order, the set of dimer states was reduced by keeping only those that were lowest in energy. In low powers of λ, the pinwheel-dimer state has one of the highest energies, as it has no resonating hexagons, and was not considered further.[8] However, all dimer states were found to be degenerate to the second order in perturbation theory and stayed within a few percent of each other for $\lambda = 1$ to the highest order studied. Thus, it is possible that higher powers of λ can stabilize a different state than the ones picked out perturbatively. Standard series expansions in λ are clearly not suitable to study such a selection.

We develop here a numerical linked-cluster expansion (NLCE)[18] to study this problem. This is a graphical method based on the principle of inclusion and exclusion for calculating the properties of an infinite system by summing over contributions from all smaller clusters. Its convergence is not based on the existence of a small parameter, but rather on having a short correlation length, so that contributions from larger clusters become small. Such an expansion always converges at high temperatures, but can also converge at low temperatures for models where the correlation length remains short.[18]

A suitably chosen NLCE scheme can also converge at $T = 0$ if the system has long-range VBC order, but the fluctuating correlation length on top of the VBC order remains small. By building the clusters in terms of the dimers of the pinwheel VBC order (see Appendix for details of the
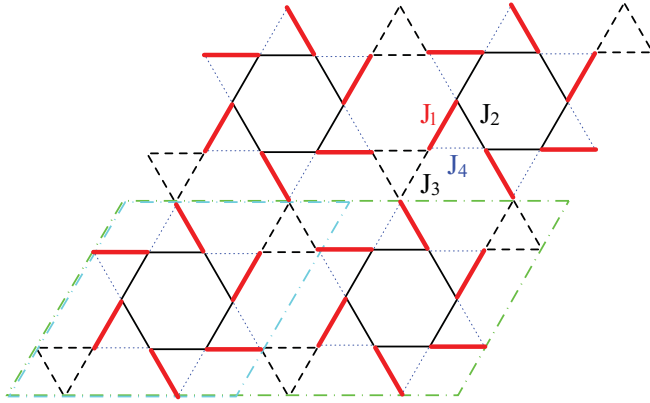
FIG. 1. (Color online) Kagome lattice with bond anisotropy as relevant to the $Rb_2Cu_3SnF_{12}$ material. The strength of the bonds (J_α) can be inferred by their thickness. Red (thick) bonds show dimers of the pinwheel VBC order with a 12-site unit cell, which is the ground state when J_1 is sufficiently larger than the other exchange interactions. The dotted-dashed lines show the 12-site and 24-site periodic clusters used in ED.

expansion), the properties of such a phase can be calculated. There is no small parameter in the expansion, as the properties of the finite clusters are calculated exactly. For concreteness, we introduce a family of models that depend on a parameter λ, defined in the same way as for the series expansion. As long as our NLCE shows internal convergence, one can study any ground-state property. The failure to converge signals a phase transition away from the VBC phase.

We first use the NLCE to study the specific heat (C_v), entropy (S), and spin susceptibility (χ) of the pinwheel distorted kagome lattice with exchange constants that describe $Rb_2Cu_3SnF_{12}$.[16,17] Our results are accurate in the thermodynamic limit and converge at almost all temperatures (including $T = 0$). They also compare very well with the experimental data for the uniform susceptibility, confirming the pinwheel valence-bond nature of the ground state of this material. We then consider a model in which the exchange constants are unity for the strong bonds in the pinwheel order and λ for all others. We study the thermodynamics of this model for λ from the dimerized ($\lambda \ll 1$) to the uniform KLHM ($\lambda = 1$). Since, sufficiently away from $\lambda = 1$, the NLCE converges at $T = 0$, we use a Lanczos-based NLCE and include larger cluster sizes to study ground-state properties (see Appendix for details). We find that a VBC order parameter decreases as λ increases and, according to a power-law fit, vanishes at $\lambda_c < 1$. The results for finite-size clusters with periodic boundary conditions point to a first-order phase transition from the VBC phase to a spin-liquid-like phase at $\lambda_c \gtrsim 0.9$.

II. THE MODEL

The KLHM Hamiltonian is written as

$$\hat{H} = \sum_{\langle ij \rangle_\alpha} J_\alpha \, \hat{\mathbf{S}}_i \cdot \hat{\mathbf{S}}_j, \qquad (1)$$

where $\langle .. \rangle$ denotes nearest neighbors, $\hat{\mathbf{S}}_i$ is the spin-1/2 vector on site i, and α is the bond type. We consider the bond anisotropy seen in Fig. 1 with four distinct α's.

III. RESULTS

A. Thermodynamics of $Rb_2Cu_3SnF_{12}$

We study the thermodynamics of the anisotropic KLHM shown in Fig. 1, with the exchange constants suggested for $Rb_2Cu_3SnF_{12}$ in a recent experiment.[17] We take $J_2 = 0.95J_1$, $J_3 = 0.85J_1$, and $J_4 = 0.55J_1$, and set the unit of energy to J_1. In Figs. 2(a)–2(c), we show results for the 8th and 9th orders of bare NLCE sums,[18] along with results from ED on a 12-site periodic cluster, for C_v, S, and χ per site. In addition to the high-T region, the thermodynamic quantities also fully converge in a low-T window between 0 and 0.1. This shows that clusters in our dimer expansion around the pinwheel VBC order are able to capture the low-T properties very well, which in turn supports the finding that this ordered phase describes the ground state of $Rb_2Cu_3SnF_{12}$.[9,17]

In Fig. 2(a), note the relatively flat C_v of this model for T between 0.1 and 1.0 [Fig. 2(a)], reminiscent of a classical gas. The entropy in that region varies almost linearly with $\log T$ [Fig. 2(b)]. The ED results for C_v exhibit a double-peak structure but clearly underestimate the value of the high-T peak as seen in Fig. 2(a). Large finite-size effects in ED can also be seen at low T in Fig. 2(c).

Figure 2(c) shows a comparison between the experimentally measured[16] χ and the NLCE results using $J_1 = 234$ K and the g factor, $g = 2.46$ (needed to match the two at high T). We find a remarkable agreement between the NLCE results within its convergence region ($T > 0.4$ and $0 < T < 0.15$) and the experiments [Fig. 2(c)]. The fact that the zero-T
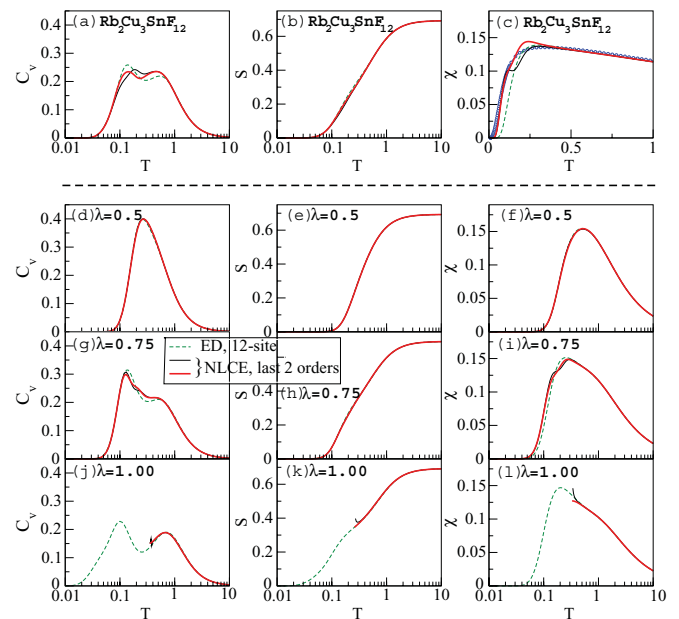

FIG. 2. (Color online) Specific heat, entropy, and uniform spin susceptibility per site for the pinwheel distorted kagome lattice of Fig. 1 with (a)–(c) $J_2 = 0.95J_1$, $J_3 = 0.85J_1$, and $J_4 = 0.55J_1$ (the model for $Rb_2Cu_3SnF_{12}$), and (d)–(l) $J_2 = J_3 = J_4 = \lambda J_1$. The last two orders of the bare sums in the NLCE are shown. They are 5th and 6th orders for $\lambda = 0.50$, and 8th and 9th orders for $\lambda = 0.75$ and $\lambda = 1.00$, and in (a)–(c). Dashed lines are results from ED for the periodic 12-site cluster. Blue circles in (c) are experimental results from Ref. 16 (see text).

fit of the spectra in Ref. 17 and the finite-T susceptibility correspond to roughly the same parameters also shows that the exchange constants are nearly temperature independent. Small deviations at $T < 0.07$ can be attributed to the uncertainty in the impurity subtraction.[16]

B. Thermodynamics of the model with $J_2 = J_3 = J_4 = \lambda J_1$

We are interested in the behavior of thermodynamic quantities and the NLCE convergence at low T for different λ values.[19] In Figs. 2(d)–2(l), we show C_v, S, and χ for $\lambda = 0.50$, 0.75, and 1.00. Figures 2(d)–2(f) show excellent convergence of the NLCE results at all T in the 5th and 6th orders for $\lambda = 0.5$. Note that the specific heat in Fig. 2(d) has a single peak at $T \sim 0.27$ with no other features, which is characteristic of a single dimer.

Upon increasing λ to 0.75, the NLCE results still converge at nearly all temperatures by increasing the order to 9. Despite this convergence, which suggests that the physics of the VBC is still dominant, the temperature dependence of the specific heat, entropy, and susceptibility changes from those of $\lambda = 0.5$. The peak in the specific heat splits into two peaks [Fig. 2(g)] and the entropy develops a hump in that region [Fig. 2(h)]. Also, the peak in susceptibility broadens and moves to lower T [Fig. 2(i)]. Unlike the $\lambda = 0.5$ case, due to finite-size effects, the 12-site ED results do not completely agree with the NLCE results when $\lambda = 0.75$, and again, underestimate the specific heat for $0.2 \lesssim T \lesssim 0.5$.

The convergence of the NLCE results changes completely in the uniform limit ($\lambda = 1$), as depicted in Figs. 2(j)–2(l). Similar to previous NLCE calculations that use the site or triangular expansions on the kagome lattice,[18] the series do not converge below $T \sim 0.3$. Hence, the low-temperature physics can no longer be described in the dimerized picture.

C. The ground state

To study ground-state properties directly, we use the Lanczos algorithm and carry out the NLCEs to the 13th order. We calculate the bond energies B_α per bond of each type in Fig. 1. The difference between B_1 and any other bond energy, e.g., $B_2 - B_1$, can be used as the order parameter. For small λ, when the system is almost completely dimerized in the pinwheel pattern, B_1 is dominant and the order parameter is maximum. As λ increases, all B_α should approach the same value, which at $\lambda = 1$ is half the ground-state energy per site. Although this order parameter can never be exactly zero for any $\lambda \neq 1$, there is the possibility of a phase transition from the bond-solid order to some other phase for $\lambda_c < 1$, beyond which the difference in bond energies arises from the difference in the exchange constants, not dimerization. Naively, the order parameter would vanish linearly with λ in this region.

In Fig. 3, we show the dependence of $B_2 - B_1$ on λ. We find very good convergence for small values of λ. However, for $\lambda > 0.85$, the bare sums in the NLCE do not converge. Resumming the series using the Wynn algorithm[18] extends the region of convergence to $\lambda \sim 0.91$ (last two orders are shown in Fig. 3). This is, in fact, an indication that a small pinwheel distortion of the kagome lattice fails to stabilize the VBC order and that there is a transition at $0.9 < \lambda_c < 1$ to another phase [presumably a spin-liquid (SL) phase] in the
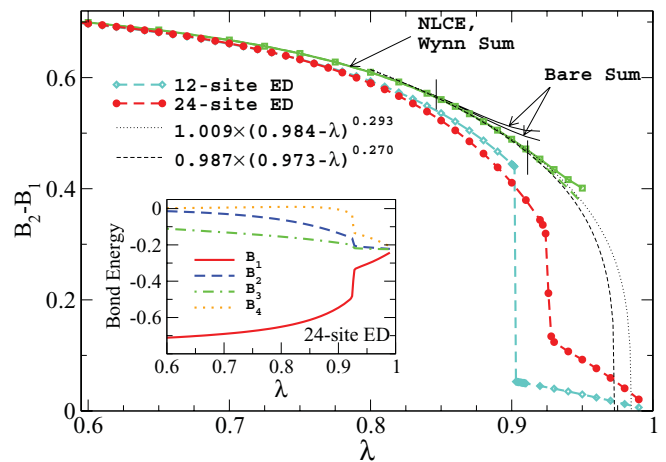

FIG. 3. (Color online) VBC order parameter at $T = 0$ vs the anisotropy parameter λ for $J_2 = J_3 = J_4 = \lambda J_1$. The results for finite-size clusters show a first-order transition. Bare NLCE sums do not converge beyond $\lambda \sim 0.85$. We use the Wynn sum with four cycles of improvement[18] to extend the convergence to $\lambda \sim 0.9$. Results for the last two orders of the former are fit to $A(\lambda_c - \lambda)^B$ (thin dotted and dashed lines). Vertical solid lines show the region used for the fit. The inset shows the four bond energies for the 24-site ED vs λ.

thermodynamic limit. In Fig. 3, we also show the ED results from the 12- and 24-site clusters for the entire region of λ. Both clusters exhibit a clear first-order transition with $\lambda_c < 1$. In the inset of Fig. 3, we show the behavior of individual bond energies for the 24-site cluster. It is interesting to see that the bond energy B_3 of the so-called "empty triangles"[8] is the least affected by the transition. We should stress that $B_2 - B_1$ in the ED results exhibit large finite-size effects in the region where the NLCE is converged, and increasing the cluster size from 12 to 24 does not improve the value of $B_2 - B_1$ for $\lambda < \lambda_c$. As one can see in Fig. 3, for $\lambda < \lambda_c$, the results from the 24-site cluster are further away from the (thermodynamic limit) NLCE results than those from the 12-site cluster.

A power-law fit of the high-λ NLCE results for the order parameter, allows us to estimate λ_c in the event of a second-order phase transition. We find $\lambda_c \sim 0.98$ when considering the last two orders of the NLCE after resummation. Results for the fit are shown as thin dotted and dashed lines in Fig. 3. If the transition is actually first order, λ_c will be smaller.

D. Order parameter at finite temperatures

Finally, in connection with the experiments, and to explore the effects of a possible quantum critical region, we use NLCEs and ED on the 12-site cluster to examine the behavior of $B_2 - B_1$ at finite T. The contour plot in the upper panel of Fig. 4 shows the order parameter in the T-λ plane obtained from the ED of the 12-site cluster. The blue area (dark area in the left) for $\lambda \lesssim 0.9$ at low temperatures indicates the VBC phase, and the red area (dark area in the right) for $\lambda \gtrsim 0.9$ belongs to the other phase. Separating these two phases is a crossover region, shown by the light color in that figure, which starts at the finite-size transition point of the 12-site cluster ($\lambda_c \sim 0.91$) and is broadened as it moves to smaller λ at higher T. We
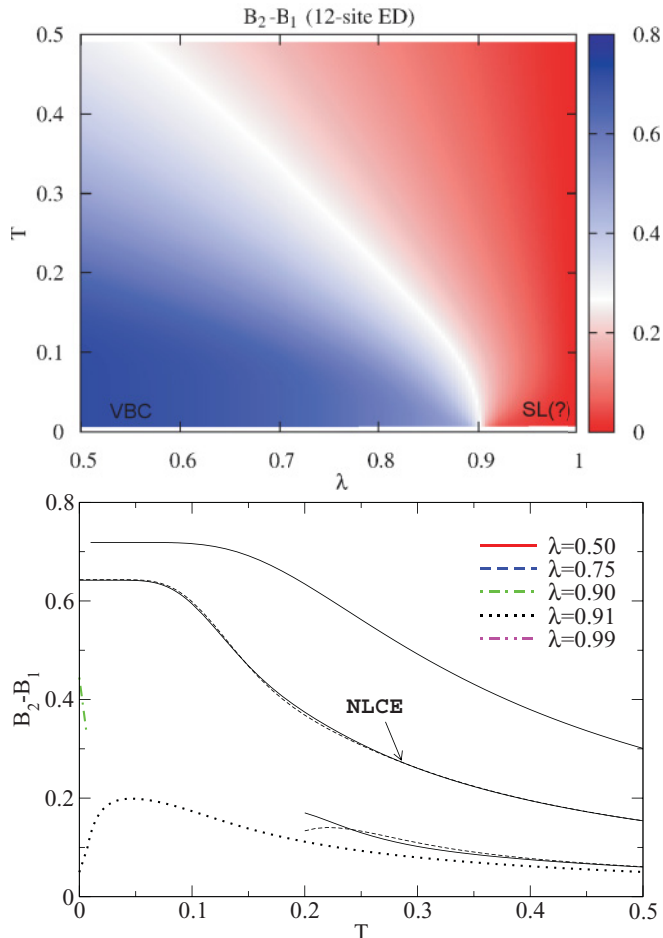
FIG. 4. (Color online) Upper panel: Plot of the VBC order parameter $B_2 - B_1$ in the T-λ plane for the 12-site ED calculations. The decrease in $B_2 - B_1$ by increasing λ from the left VBC region to the right region is less abrupt at higher temperatures. Lower panel: The same quantity vs T for five different values of λ below and above the transition point. Thin lines are the 7th and 8th order NLCE, and thick lines are the results for the 12-site cluster.

expect the same qualitative behavior in the thermodynamic limit, with a transition point that is closer to the $\lambda = 1$ axis.

To compare with the NLCE results, in the lower panel of Fig. 4, we plot the order parameter for different values of λ below and above the transition point. An interesting feature there is the initial low-temperature rise of the order parameter above but very close to λ_c as T is increased from zero. In this region, thermal fluctuations initially increase the value of the order parameter before suppressing it at higher T. If the transition in the thermodynamic limit is second order or weakly first order and closer to $\lambda = 1$, there could be a quantum critical region that controls the temperature dependence of the KLHM over some temperature range.[14]

IV. SUMMARY

In summary, we have studied the KLHM on a pinwheel distorted kagome lattice using NLCEs and exact diagonaliza-

tion of finite clusters. We have examined the thermodynamic properties of the model with exchange parameters appropriate for $Rb_2Cu_3SnF_{12}$, and obtained results that are consistent with the experimental observations. We have also developed a Lanczos-based NLCE and studied the approach to the uniform KLHM at $T = 0$ in such a pinwheel-dimerized system. We find strong evidence for a phase transition before the uniform limit is reached, implying that the KLHM may not spontaneously dimerize in this pattern and its ground-state phase is stable to small pinwheel distortions.

APPENDIX: NUMERICAL LINKED-CLUSTER EXPANSION FOR THE DISTORTED KAGOME LATTICE

In standard series expansions for the distorted kagome-lattice Heisenberg models,[8] the ground-state properties of each cluster in the series are calculated using perturbation theory in the small parameter, λ. The contributions of all of the clusters, up to a certain size, to each power of λ are then added properly into the series. In contrast, in the NLCEs, the property of each cluster is computed exactly, i.e., to all orders of λ, using exact diagonalization techniques.[18] Because of this, the NLCE does not require λ to be small, and one can achieve convergence in a region that extends beyond that of the usual series expansions. The convergence in NLCEs is controlled by the relevant correlation length in the system. Hence, unlike for standard series expansions, by adding larger cluster sizes, we can always improve the convergence.

In our expansion, the building blocks for generating the linked clusters are dimers of the pinwheel VBC. This means that in the nth order, we generate all of the clusters with n dimers that can be embedded in the anisotropic kagome lattice (Fig. 1). Starting from a single dimer in the first order, there are many possibilities for the topology of the clusters in the second order, generated by adding another neighboring dimer. However, among those, only the four clusters shown in Fig. 5 are topologically distinct.[20] Next, we require that dimers be connected only through *complete triangles*. For example, in the second order, we consider only cluster D among those in Fig. 5. The above condition significantly reduces the number of clusters we have to diagonalize in higher orders, while still capturing the fundamental physics at low energies in
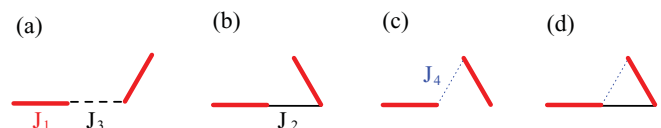

FIG. 5. (Color online) All possible configurations for two neighboring dimers (red thick bonds) on a kagome lattice with pinwheel anisotropy. In general, four different types of bonds, $J_1, \ldots, J_4$, can be distinguished in this lattice. Cluster D, in which the two dimers are connected via a complete triangle, is the only cluster considered in the second order of our expansion.
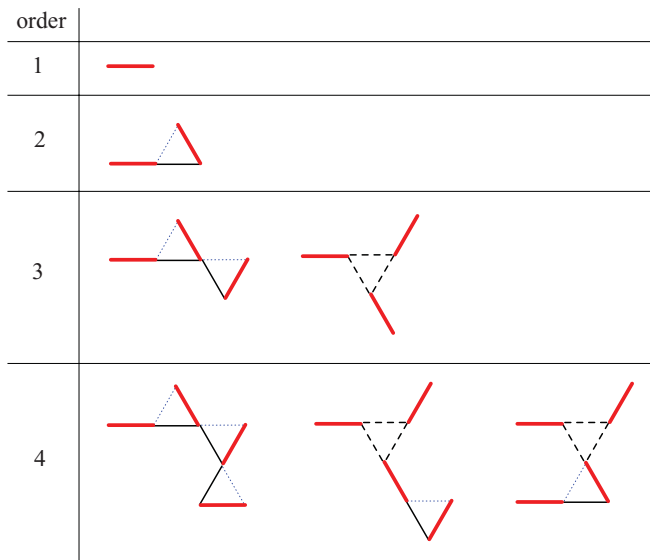
FIG. 6. (Color online) All the topologically distinct clusters up to the fourth order in our expansion. Bond types are the same as in Fig. 5.

TABLE I. Number of topologically distinct clusters up to the 13th order of the expansion.

Order No.	1	2	3	4	5	6	7	8	9	10	11	12	13
No. of clusters	1	1	2	3	7	14	25	50	102	216	442	929	1969

algorithm to access its ground state only. The advantage of the latter is that it enables us to deal with systems with much larger Hilbert spaces, and so we are able to carry out the expansion to significantly larger orders in comparison to the finite-temperature case.

Computationally, the dominant part of the calculations is the diagonalization step in the last order. Ultimately, we are limited either by the large number of clusters that exist in the largest order we consider and the computational time it takes to solve for each of them, or by memory requirements for diagonalizing the Hamiltonian of each of those clusters. For the full diagonalization finite-temperature calculations, we consider clusters up to the 9th order, and for zero-temperature Lanczos calculations, up to the 13th order. Hence, only in the last order of the former case, 102 clusters need to be solved. Each of them has 18 sites and, therefore, the size of the Hilbert space for the largest spin sector (with equal number of spin-ups and spin-downs) is $\binom{18}{9} = 48\,620$. The large memory requirements for the calculation of the full spectrum, needed for the finite-temperature NLCE, is the one that limits our expansion to the 9th order in this case.

For the ground-state calculations, we consider clusters up to the 13th order. Here, only in the last order, 1969 clusters have to be diagonalized. Each of them has 26 sites and the size of the Hilbert space for the largest spin sector is $\binom{26}{13} = 10\,400\,600$. The memory requirements for these calculations are much smaller than those for the full diagonalization (only three vectors of this size need to be stored at any given time). What limits our ground-state expansion to the 13th order is the time they take to converge in the Lanczos loop, so that the ground-state energy is obtained with a relative accuracy of 10^{-14} for orders less than or equal to 12 and of 10^{-9} for the 13th (last) order. The convergence requirements that are imposed guarantee at least 5-digit accuracy for the final observables after summing the contributions of all of the clusters.

relatively short expansions. This selection of the clusters offers a consistent scheme for the linked-cluster expansion of the infinite lattice. Following the same process, we end up with two topologically distinct clusters in the third order by adding the next dimer, and so on. The clusters in the series, up to the fourth order, are depicted in Fig. 6. In Table I, we have listed the number of topological clusters in each order up to the 13th order.

The expansion described above offers a unique approach in which the series capture not only the high-temperature physics, like the standard NLCEs used previously,[18,21] but also capture the low-temperature physics very well, as long as the pinwheel VBC is the ground state. This makes the NLCE used in this work fundamentally different from the ones implemented before. It uses a basis tailored to describe the ground state of this particular model. Hence, we use it to calculate properties both at finite temperatures and, specially, at zero temperature. For finite-temperature calculations, we compute the full spectrum of the Hamiltonian for every cluster in the series using standard full diagonalization techniques, and for zero-temperature calculations, we employ the Lanczos

[1] C. Lhuillier, e-print arXiv:cond-mat/0502464 (to be published); G. Misguich and C. Lhuillier, in *Frustrated Spin Systems*, edited by H. T. Diep (World Scientific, Hackensack, NJ, 2004).

[2] D. A. Huse and A. D. Rutenberg, Phys. Rev. B **45**, 7536 (1992).

[3] R. R. P. Singh and D. A. Huse, Phys. Rev. Lett. **68**, 1766 (1992).

[4] P. Sindzingre and C. Lhuillier, Europhys. Lett. **88**, 27009 (2009).

[5] P. Sindzingre, G. Misguich, C. Lhuillier, B. Bernu, L. Pierre, Ch. Waldtmann, and H.-U. Everts, Phys. Rev. Lett. **84**, 2953 (2000).

[6] F. Mila, Phys. Rev. Lett. **81**, 2356 (1998).

[7] C. Zeng and V. Elser, Phys. Rev. B **42**, 8436 (1990); J. B. Marston and C. Zeng, J. Appl. Phys. **69**, 5962 (1991); S. Sachdev, Phys. Rev. B **45**, 12377 (1992); P. W. Leung and V. Elser, *ibid.* **47**, 5459 (1993); M. B. Hastings, *ibid.* **63**, 014413 (2000); A. V. Syromyatnikov and

S. V. Maleyev, *ibid.* **66**, 132408 (2002); P. Nikolic and T. Senthil, *ibid.* **68**, 214415 (2003); R. Budnik and A. Auerbach, Phys. Rev. Lett. **93**, 187205 (2004); Y. Ran, M. Hermele, P. A. Lee, and X.-G. Wen, *ibid.* **98**, 117205 (2007); F. Wang and A. Vishwanath, Phys. Rev. B **74**, 174423 (2006); H. C. Jiang, Z. Y. Weng, and D. N. Sheng, Phys. Rev. Lett. **101**, 117203 (2008); Z. Hao and O. Tchernyshyov, *ibid.* **103**, 187203 (2009); G. Evenbly and G. Vidal, *ibid.* **104**, 187203 (2010); D. Poilblanc, M. Mambrini, and D. Schwandt, Phys. Rev. B **81**, 180402 (2010).

[8] R. R. P. Singh and D. A. Huse, Phys. Rev. B **76**, 180407 (2007); **77**, 144415 (2008).

[9] B.-J. Yang and Y. B. Kim, Phys. Rev. B **79**, 224417 (2009).

[10] S. Yan, D. A. Huse, and S. R. White, Science **332**, 1173 (2011).

[11]H. Fukuyama, J. Phys. Soc. Jpn. **77**, 111013 (2008).

[12]J. S. Helton, K. Matan, M. P. Shores, E. A. Nytko, B. M. Bartlett, Y. Yoshida, Y. Takano, A. Suslov, Y. Qiu, J.-H. Chung, D. G. Nocera, and Y. S. Lee, Phys. Rev. Lett. **98**, 107204 (2007); A. Olariu, P. Mendels, F. Bert, F. Duc, J. C. Trombe, M. A. de Vries, and A. Harrison, *ibid.* **100**, 087202 (2008); T. Imai, E. A. Nytko, B. M. Bartlett, M. P. Shores, and D. G. Nocera, *ibid.* **100**, 077203 (2008); M. A. de Vries, K. V. Kamenev, W. A. Kockelmann, J. Sanchez-Benitez, and A. Harrison, *ibid.* **100**, 157205 (2008); A. Zorko, S. Nellutla, J. van Tol, L. C. Brunel, F. Bert, F. Duc, J.-C. Trombe, M. A. de Vries, A. Harrison, and P. Mendels, *ibid.* **101**, 026405 (2008).

[13]F. Bert, D. Bono, P. Mendels, F. Ladieu, F. Duc, J.-C. Trombe, and P. Millet, Phys. Rev. Lett. **95**, 087203 (2005).

[14]M. Rigol and R. R. P. Singh, Phys. Rev. Lett. **98**, 207204 (2007); Phys. Rev. B **76**, 184403 (2007).

[15]O. Cépas, C. M. Fong, P. W. Leung, and C. Lhuillier, Phys. Rev. B **78**, 140405 (2008).

[16]K. Morita, Midori Yano, Toshio Ono, Hidekazu Tanaka, Kotaro Fujii, Hidehiro Uekusa, Yasuo Narumi, and Koichi Kindo, J. Phys. Soc. Jpn. **77**, 043707 (2008).

[17]K. Matan, T. Ono, Y. Fukumoto, T. J. Sato, J. Yamaura, M. Yano, K. Morita, and H. Tanaka, Nature Phys. **6**, 865 (2010).

[18]M. Rigol, T. Bryant, and R. R. P. Singh, Phys. Rev. Lett. **97**, 187202 (2006); Phys. Rev. E **75**, 061118 (2007).

[19]Note that our model differs from Ref. 9 in which a $J_1 = J_2 = J_3 > J_4$ pattern is considered for exchanges.

[20]Note that when adding a dimer, we always increase the size of the cluster by 2; all clusters in the nth order have $2n$ sites.

[21]E. Khatami and M. Rigol, Phys. Rev. B **83**, 134431 (2011).